Field technique of permeability tests in highly fissured limestone strata

Adnan Al-Salihi · Abdulah Asaad

Abstract A design of a dewatering system is necessary for site improvement prior to the construction of some structures. The design of an efficient dewatering system requires estimating the value of the in-situ coefficient of permeability. The available relationships for estimating the permeability coefficient were developed based on limited field measurements and conditions, and their predictions vary by several orders of magnitudes. Therefore, it was necessary to conduct field measurements of permeability and determine the relationship that best fits these measurements prior to the design of a dewatering system for specific geological and site conditions.

This paper presents field measurements of permeability in complex chaotic and diagenetic limestone strata. It also offers comparative analysis of several relationships available in the literature for predicting the in-situ coefficient of permeability. The analysis is conducted for both steady and nonsteady conditions. The results show that the coefficient of permeability value is dependent on the water table level, which is affected by the tidal condition. The US Navy equation is shown to give the best correlation with field measurements.

Résumé L'étude de dispositifs de dénoyage est nécessaire pour l'amélioration de sites avant la construction de certaines structures. L'étude de dispositifs de dénoyage efficaces exige d'estimer la valeur du coefficient de perméabilité in situ. Les relations disponibles pour estimer le coefficient de perméabilité ont été développées sur la base de mesures et de conditions de terrain limitées, et les prédictions varient de plusieurs ordres de grandeur. C'est pourquoi il est nécessaire de réaliser des mesures de perméabilité sur le terrain et de déterminer la relation qui permet le meilleur ajustement de ces mesures avant l'étude du dispositif de dénoyage pour des conditions locales et géologiques spécifiques. Ce papier présente des mesures de perméabilité sur le terrain dans des niveaux calcaires complexes chaotiques et diagénétisés. Il propose également une analyse comparative de plusieurs relations disponibles dans la littérature destinées à prédire le coefficient de perméabilité in situ. L'analyse est faite en conditions permanentes et non permanentes. Les résultats montrent que la valeur du coefficient de perméabilité dépend du niveau de la nappe, qui est affecté par le régime de marées. On montre que l'équation de l'US Navy donne la meilleure corrélation avec les mesures de terrain.

Resumen El diseño de sistemas de desecado es necesario para mejorar las condiciones de un emplazamiento antes de la construcción de determinadas estructuras. El diseño de un sistema eficiente de desecado requiere de la estimación del valor de la permeabilidad in-situ. Las relaciones disponibles para tal fin han sido desarrolladas bajo condiciones y medidas de campo limitadas; sus predicciones varían en algunos órdenes de magnitud. Por tanto, es necesario tomar medidas de permeabilidad en campo y determinar la relación que reproduce mejor dichas medidas como paso previo al diseño de un sistema de desecado en condiciones geológicas y de emplazamiento específicas. Este artículo presenta medidas de permeabilidad en campo para estratos de calcita caóticos y diagenéticos. También ofrece un análisis comparativo de diversas relaciones disponibles en la bibliografía con el fin de predecir el valor de la permeabilidad in-situ. El análisis se ha hecho tanto en régimen permanente como en estacionario. Los resultados demuestran que la permeabilidad depende del nivel freático, el cual está afectado por las mareas. La ecuación de la Marina estadounidense es la que proporciona una mejor correlación con las medidas de campo.

Keywords Coastal aquifers · Dewatering · Hydraulic properties · Tidal effects

Received: 23 October 2000 / Accepted: 6 March 2002
Published online: 23 May 2002

A. Al-Salihi (✉) · A. Asaad
Department of Civil Engineering, University of Jordan,
Amman 11942, Jordan
e-mail: mazin@go.com.jo
Tel.: +962-6-5355000 ext. 2733, Fax: +962-6-5355588

Introduction

Construction of buildings or other structures like powerhouses, dams, tunnels and gravity docks often require excavation below the water table into water-bearing

 DOI 10.1007/s10040-002-0205-9

soils. This excavation requires lowering the water level below the bottom of the excavation to ensure dry and firm working conditions for construction operations. Sometimes the excavation may be underlain by a stratum under artesian pressure, which, if not relieved, can rupture the foundation.

Groundwater may be controlled by means of one or more types of dewatering systems appropriate to the size and depth of the excavation, geological conditions and characteristics of the stratum. In determining the need for and before selecting and designing a successful dewatering system, the soil conditions should be investigated. The permeability of the strata to be dewatered or in which the hydrostatic pressure is to be reduced should be determined prior to designing an efficient dewatering system, as dictated by the British Standards BS 8004 (1986).

Various methods may be used to determine this permeability. Laboratory permeability tests cannot be used for some strata because they give results not indicative of the actual in-situ permeability. For large dewatering projects a pumping test is warranted to determine the permeability of the pervious formation. The tested formation in this research has unique characteristics. Therefore, the well test and the governing equations are of special interest.

Constructing dewatering systems for a large area comprising rings of closely spaced wells may be modelled as equivalent to a large single well (Cedergren 1989; Powers 1992). There is normally no need to consider in detail the flow to individual wells at the initial stage of the design process, and the drawdown in the equivalent well is taken as the required drawdown over the area of the excavation (Preene and Powrie 1993). In case a confined aquifer and a fully penetrating circular well is assumed, simple formulae may be used to relate the pumped flow rate to the drawdown, the aquifer permeability, the distance to the recharge boundary and the size of the well (Powrie and Preene 1992).

Site Description and Conditions

A dewatering system needs to be designed prior to the construction of the museum of Islamic Arts. This museum is to be constructed on a triangular site area that measures approximately 11 ha and slopes gently from an elevation of 6 m down to 2 m towards the Gulf. It is located at Doha-capital of Qatar that lies midway along the eastern coast of the Qatar peninsula (see Fig. 1).

The total area for the proposed museum buildings is 83,283 m^2. The basement is comprised of areas 1 and 2 with 24,124 and 22,219 m^2 respectively. The depth of excavation for the above-mentioned basements varies between 4 and 7 m below ground surface. The average foundation level is around 3.0 m below the Qatar National Datum (QND 0.9 m below average Gulf-water level). The intended use of the basement is to house the invaluable Islamic art collections. Hence, the basement must be designed as a watertight structural system against the potential Gulf-water intrusion.

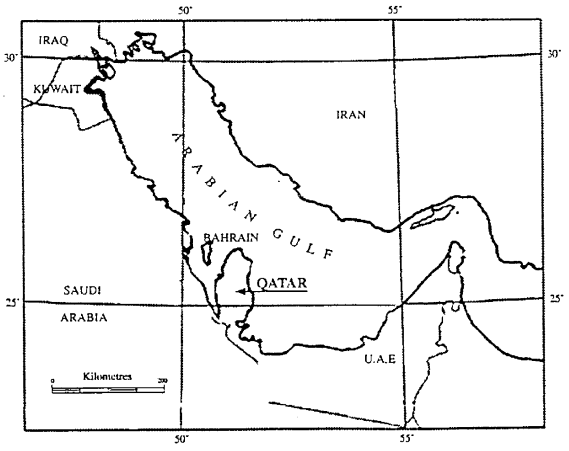

Fig. 1 Geographical location

The most appropriate kind of dewatering system for a given job depends not only on the size and depth of the excavation, the amount of lowering the water table and the length of time the excavation must be maintained in a dewatered condition, but, to a large extent, on the properties of the soil formations. For an effective dewatering system, detailed soil and geological investigations should always be made. Careful investigations are needed to identify sources of replenishment of the groundwater regime as well as the capability of the aquifer to be replenished.

Field investigations (Arab Centre 1998; Gulf Labs 1998; Qatar Industrial Labs 1998) revealed that partially consolidated fill of varying depth (0.9–2 m) overlays limestone of the Simsima Member of the Upper Dammam subformation (Eocene age – approximately 45–55 million years old). The fill was introduced during a reclamation programme carried out during the 1970s. The limestone possesses a bimodal nature comprising hard recrystallised predominantly calcareous (occasionally dolomitic) 'original' limestone and a variable percentage of secondary attapulgitic mudstone/clay/siltstone.

The Simsima limestone encountered on the site is a complex chaotic and diagenetic limestone and consists of creamy, off-white to pale brown, red and bluish grey slightly to heavily fractured (Akili and Jackson 1998). Occasionally pseudo brecciated, weak to strong, medium-grained chalky or crypto-crystalline dolomitic to calcareous limestone with numerous pockets of soft off-white pale green, and iron-stained diagenetically derived carbonate siltstone and attapulgitic clay was encountered. The blue grey limestone frequently contained horizontal to subhorizontal cavities 2 to 75 mm in diameter often lined with calcareous silty sand or massive fibrous gypsum (Domenico and Schwartz 1998). Figure 2 clearly shows the large amount of lateral seepage through such cavities.

Dewatering problems in limestone and coral and shelly sandstone can range from minor to very severe. It

 DOI 10.1007/s10040-002-0205-9

is difficult to evaluate the situation by test drilling alone. The cavernous nature of the rock creating the problem usually does not appear in the cores. Poor recovery indicates the possibility of a severe problem, but does not confirm it. Also, the problems in these formations tend to be concentrated in relatively small areas; unless a large number of borings are made, the problem may be missed. A pumping test can be helpful in evaluating the extent of the problem (Powers 1992).

The permeability of water-bearing formations can also be estimated from constant or falling head tests made in wells or piezometers in a manner similar to laboratory permeameter tests. Because these tests are sensitive to details of the installation and execution of the test, exact dimensions of the well screen and casing, filter surrounding the well screen and the rate of inflow or fall in water level, all must be accurately measured (Dept. of Army, Navy, and Air Force 1983).

Field tests in a trial pit that was constructed during November and December of 1998 (Fig. 3) were considered to be the most appropriate technique to investigate the groundwater hydrology. In-situ permeability tests were carried out. Analyses of collected results and assessment of the implications on the design of the dewatering system are presented.

Fig. 2 General view of the trial pit with submersible pump

Fig. 3 Lateral flow through fissure A at the northern side wall

In-Situ Measurements of Field Permeability

The trial pit, located at 250 m from the nearest point to the Gulf, was excavated to a final depth of 6.5 m with a cross-sectional area of 30.10 m^2. A schematic diagram of the trial pit is presented in Fig. 4.

An old cased borehole, 33.45 m away from the trial pit, was used to monitor the groundwater levels over the test period, as shown in Fig. 5. The groundwater levels were measured using a steel tape attached to a probe with an electric sounder.

Following the recommendations by Driscoll (1989), the permeability field test was carried out in two stages. In the first stage, the flow area consisted of four side walls in addition to the base floor, with a total area of 113.9 m^2. The 83.8-m^2 side walls contributed lateral flow, where as the 30.10-m^2 base floor contributed upward flow. The southern side wall was absolutely dry because of the presence of the sediments sealing all existing fissures (Fig. 6).

Table 1 presents the main characteristics of the observed fissures together with the calculated approximate hydraulic gradient at three different conditions: dry bed,

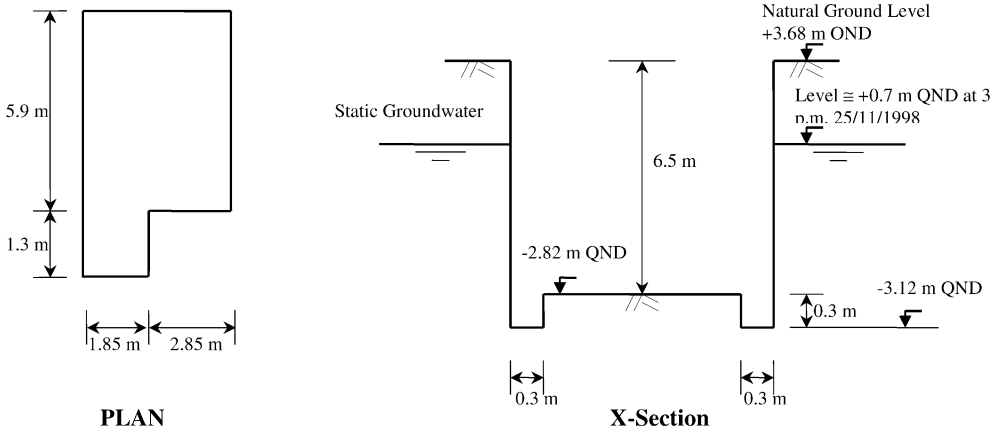

Fig. 4 Plan and cross section of the trial pit

DOI 10.1007/s10040-002-0205-9

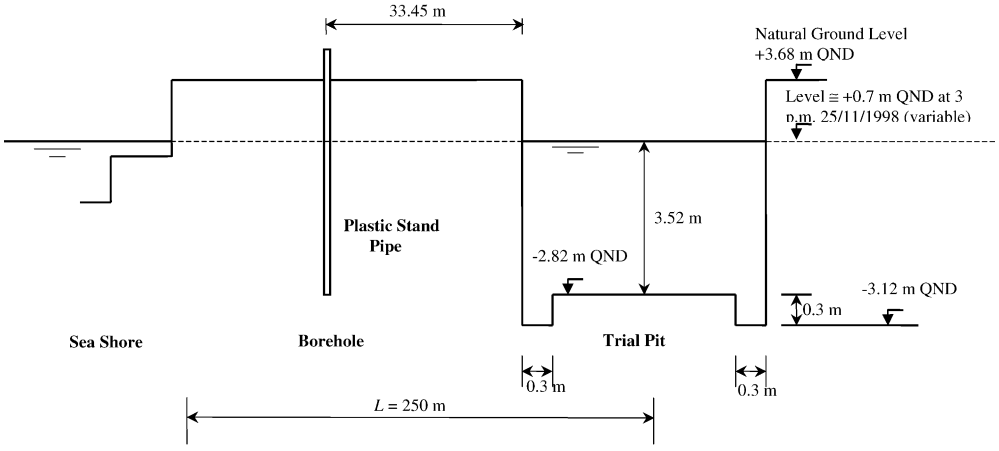

Fig. 5 Schematic profile of the trial pit together with the borehole and seashore

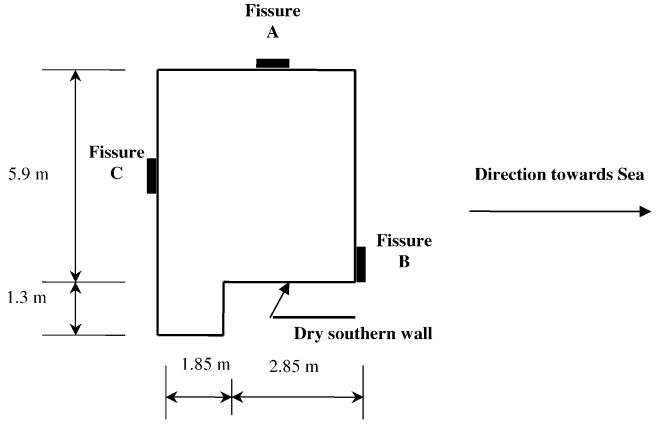

Fig. 6 Locations of the observed fissures on side walls

Fig. 7 Measurement of water levels, in the nonsteady-state condition

Table 1 Fissures' flow characteristics

Fissure	Approximate dimensions (mm)	Elevation (m QND)	Flow discharge (l/h)	Flow velocity (m/s)	Approximate hydraulic gradient (%)
A	95×60	–1.820	3,996	0.195	5.9
B	200×20	–1.620	2,700	0.187	5.4
C	145×10	–0.420	613	0.117	2.2

water level in the borehole +0.390 m QND and approximate sea level +1.130 m QND. The analysis included steady- and nonsteady-state conditions. The steady-state condition was established at four different levels: +0.535, +0.445, –1.320 and –1.670 m QND. A combination of pumps and meters was used to achieve the steady-state condition and flow measurements. Table 2 shows the recorded flow volumes for the first two water levels in addition to the coefficient of permeability calculated by Darcy's law. For the other two levels, the flow was estimated using the free jet trajectory method. The results for the steady-state condition are shown in Table 3.

The nonsteady-state condition test was carried out through a filling process, starting from dry pit at level –2.820 m QND and reaching the level +0.530 m QND with an incremental water level increase of 10 cm. The results for the nonsteady-state condition are shown in Table 4. Figure 7 shows the measurement process of water level in the trial pit. Maximum filling velocity was 1.11×10^{-3} m/s under dry pit conditions, whereas the minimum was 5.68×10^{-5} m/s at the +0.480 m QND level. Hence, the average filling velocity was estimated as 7.29×10^{-4} m/s.

In the second stage of measurements, about 0.5-m-thick reinforced concrete walls were cast to seal all side walls of the pit. The concrete side walls reduced the flow area to only 16.0 m^2. Visual inspection showed water flowing from a few small locations close to the middle of the bottom of the pit. As was done in the first stage, the results were obtained for steady and nonsteady-state conditions. In the steady-state condition, two different water

 DOI 10.1007/s10040-002-0205-9

Table 2 Steady-state flow measurements at +0.535 and +0.445 m QND water levels

Water level at pit (m QND)	Recorded volume at 5-min periods (m^3)	Average pumping flow (m^3/h)	Groundwater level at borehole (m QND)	Estimated permeability k (m/s)	Approximate seawater level (m QND)
+0.535	0.750 0.751 0.745	8.984	+0.460	2.7×10^{-4}	+1.500
+0.445	1.685 1.568 1.570	18.828	+0.420	6.3×10^{-4}	+1.340

Table 3 Steady-state flow measurements at –1.320 and –1.670 m QND water levels

Water level at pit (m QND)	Trajectory distance (m)	Average pumping flow (m^3/h)	Groundwater level at borehole (m QND)	Estimated permeability k (m/s)	Approximate seawater level (m QND)
–1.320	0.618 0.585	72.8	+0.435	1.45×10^{-3}	+0.840
–1.670	0.873 0.824	102.7	+0.415	1.99×10^{-3}	+0.750

Table 4 Nonsteady-state condition test results

Water level (m QND)		Time interval (min)	Groundwater level at borehole (m QND)	Estimated sea level[a] (m QND)	Estimated filling velocity (m/s)
From	To				
–2.820	–2.720	1.50		1.010	1.11E-03
–2.720	–2.620	1.50		1.007	1.11E-03
–2.620	–2.520	1.50		1.003	1.11E-03
–2.520	–2.420	2.00		1.000	8.33E-04
–2.420	–2.220	3.50		0.996	9.52E-04
–2.220	–2.120	2.33		0.988	7.15E-04
–2.120	–2.020	1.92		0.983	8.68E-04
–2.020	–1.920	1.83	0.290	0.978	9.11E-04
–1.920	–1.820	1.67		0.974	9.98E-04
–1.820	–1.720	1.50		0.960	1.11E-03
–1.720	–1.620	2.50		0.954	6.67E-04
–1.620	–1.520	2.50		0.949	6.67E-04
–1.520	–1.420	2.00		0.944	8.33E-04
–1.420	–1.320	2.00		0.940	8.33E-04
–1.320	–1.220	1.92		0.936	8.68E-04
–1.220	–1.120	2.00		0.931	8.33E-04
–1.120	–1.020	2.02		0.927	8.25E-04
–1.020	–0.920	2.05		0.922	8.13E-04
–0.920	–0.820	1.98		0.918	8.42E-04
–0.820	–0.720	2.20	0.390	0.913	7.58E-04
–0.720	–0.620	2.23		0.908	7.47E-04
–0.620	–0.520	2.27		0.903	7.34E-04
–0.520	–0.420	2.37		0.898	7.03E-04
–0.420	–0.320	2.52	0.430	0.892	6.61E-04
–0.320	–0.220	2.57		0.886	6.49E-04
–0.220	–0.120	2.80		0.880	5.95E-04
–0.120	–0.020	3.08		0.873	5.41E-04
–0.020	0.080	3.33		0.866	5.01E-04
0.080	0.180	3.83	0.420	0.857	4.35E-04
0.180	0.280	4.67		0.847	3.57E-04
0.280	0.380	6.17		0.833	2.70E-04
0.380	0.480	10.33		0.810	1.61E-04
0.480	0.530	14.67	0.410	0.778	5.68E-05

[a] According to tides data, Doha calendar – climate section

 DOI 10.1007/s10040-002-0205-9

Table 5 Steady-state test after concrete wall casting

Water level at pit (m QND)	Volume at 30-min periods (m^3)	Average pumping flow (m^3/h)	Groundwater at borehole (m QND)	Estimated permeability k (m/s)
–0.900	0.0513	0.1026	+0.380	0.52×10^{-4}
–0.980	0.0420	0.0840	+0.370	0.40×10^{-4}

Table 6 Nonsteady-state test results after concrete wall casting

Water level (m QND)		Groundwater level at borehole (m QND)	Estimated filling velocity (m/s)
From	To		
–2.470	–2.150		7.62E-05
–2.150	–1.890	0.340	6.19E-05
–1.890	–1.710		4.29E-05
–1.710	–1.500		5.00E-05
–1.500	–1.370		3.10E-05
–1.370	–1.220		3.57E-05
–1.220	–1.080		3.33E-05
–1.080	–0.930	0.380	3.57E-05

levels –0.900 and –0.980 m QND were maintained through continuous pumping. Table 5 shows the recorded volumes. For the nonsteady-state condition (recovery), the test started at the water level of –2.470 m QND. An incremental time interval of 70 min was adopted to monitor the water level rising up to –0.930 m QND. The results of the nonsteady-state condition are given in Table 6.

Analysis and Results

Previous investigators have developed with various relationships to calculate the rate of flow and the coefficient of permeability under various test assumptions. The measurements for both the steady- and nonsteady-state conditions obtained from this study are compared with the predictions of some of the available relationships. For the steady-state condition, the site aquifer revealed a unique condition that can be modelled by radial flow in a mixed confined and water table aquifer. The rate of flow for such a case can be estimated by the equation suggested by Mansur and Kaufman (1962):

$$q = \frac{\pi k\left[(H-s)^2 - t^2\right]}{2.303\log(R/r_w)}\left[1 + \left(0.3 + \frac{10r_w}{H}\right)\sin\frac{1.8s}{H}\right] \qquad (1)$$

where the notations in the above equation are shown in Fig. 8.

Equation (1) was developed for site conditions similar to the ones investigated in this study. However, a discrepancy revealed in the results can be attributed to special strata characteristics. A geological study (Gulf Labs 1998) showed that the depth below the bottom of the trial pit to an impermeable layer (s) was roughly 30 m. In the presence of a recharge source (Gulf), the equivalent radius of influence (R) was equal to $2L$ (Powers 1992). L was estimated as 250 m as shown in Fig. 5. H was estimated according to groundwater fluctuation attributed to the tide curve (Fetter 1988; Vuković and Soro 1992). The data collected from piezometer readings, together with seawater level analysis (Doha calendar-climate section, Department of Civil Aviation and Meteorology 1998), was used to develop Fig. 9. As expected, the tide in the aquifer is lagging behind the tide in the Gulf and has lower amplitude.

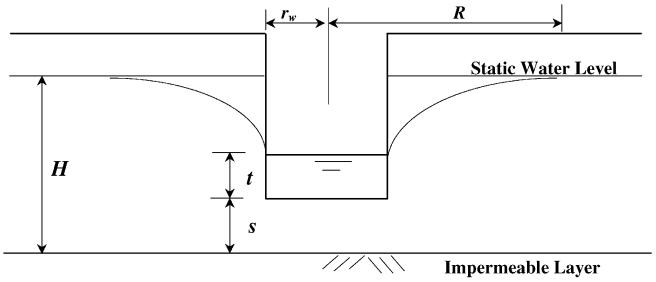

Fig. 8 Schematic diagram for Mansur and Kaufman relation

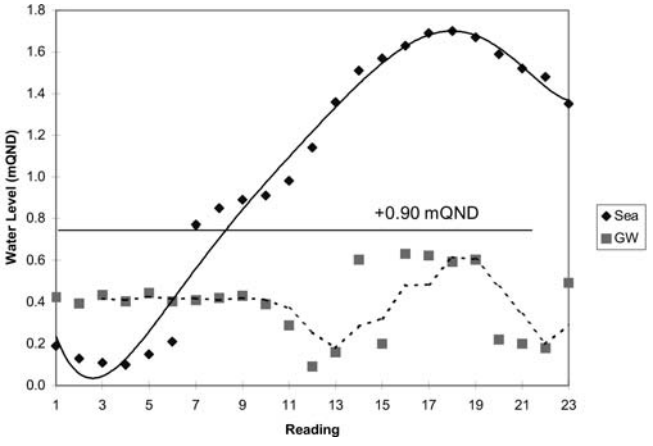

Fig. 9 Effect of tidal variation on water-table level

Table 7 presents the estimates of the coefficient of permeability according to Eq. (1). In the modelling of a dewatering system as an equivalent well, both the geometry of the excavation and the distance to an idealised recharge boundary condition must be considered. Rectangular wells can be modelled as equivalent circular wells provided that the distance to recharge is large compared with the size of the excavation (Preene and Powrie 1993). The permeability was calculated for two different equivalent radii (r_w; Powers 1992): first, based on the same cross-sectional area, as:

 DOI 10.1007/s10040-002-0205-9

Table 7 Permeability at steady-state conditions according to Mansur and Kaufman (1962)

q (m^3/h)	H (m)	t (m)	k (m/h)	k (m/s)
r_w=3.097 m (same area)				
8.984	34.32	3.355	0.891	2.48E-04
18.828	34.16	3.265	2.078	5.77E-04
72.800	33.66	1.500	4.764	1.32E-03
102.700	33.57	1.150	6.550	1.82E-03
r_w=3.788 m (same perimeter)				
8.984	34.32	3.355	0.784	2.18E-04
18.828	34.16	3.265	1.828	5.08E-04
72.800	33.66	1.500	4.188	1.16E-03
102.700	33.57	1.150	5.758	1.60E-03

L=250 m; area=30.135 m^2; perimeter=23.8 m; R=2L=500 m; r_w=3.097 m (same area), 3.788 m (same perimeter); s=30 m (depth to impermeable layer)

$$r_w = \sqrt{x - \text{sec. area}/\pi} = \sqrt{30.135/\pi} = 3.097\ \text{m}$$

or same perimeter, as:

$$r_w = \frac{\text{Perimeter}}{2\pi} = \frac{23.8}{2\pi} = 3.788\ \text{m}$$

Figure 10 clearly shows that test results in Tables 2 and 3 compare quite well with the calculated permeability shown in Table 7. This agreement is explained by the fact that Eq. (1) was derived for a porous media, and a given value of drawdown of the water level in the borehole. Therefore, yield is expected to increase as the diameter of the borehole increases. In a fissured aquifer similar to the one investigated in this study, such an increase will not materialise if no additional fissures are intercepted. Statistical analysis provided by Ineson (Henry 1986) indicated that, in general, the influence of diameter on yield is greater in fissured aquifers than in porous aquifers. He evolved the following relative values of yield for equal drawdown shown in Table 8, taking the yield of a borehole 0.46 m in diameter as unity. Figure 11 shows the yield difference normalised to diameter change; the results explain the necessity of a large hole diameter in order to predict a realistic coefficient of permeability of such fissured strata.

For the nonsteady-state condition (recovery), the single auger hole technique 'originally developed by Hooghoudt' was adopted for the evaluation of the coefficient of permeability in the trial pit. Three different equations were used for the estimate of the in-situ coefficient of permeability (Cedergren 1989).

$$k = \frac{r_w\left(\frac{r_w D}{0.19}\right)}{(2D + r_w)\,\Delta t} \ln\frac{h_1}{h_2} \qquad (2)$$

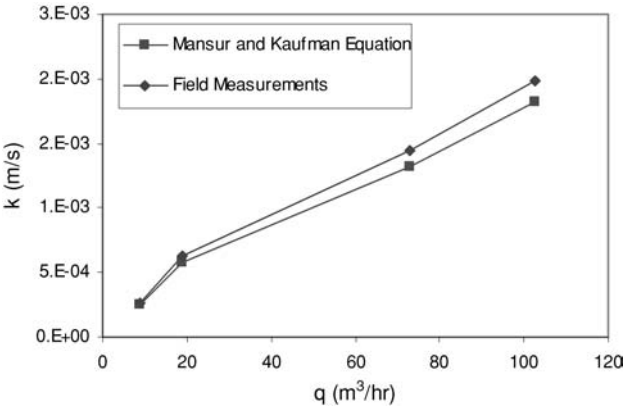

Fig. 10 Coefficient of permeability field measurement comparison with Mansur and Kaufman under steady-state conditions

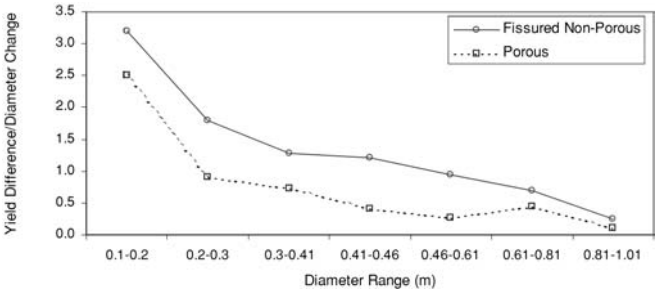

Fig. 11 Normalised yield difference to diameter change ratio at different borehole diameters

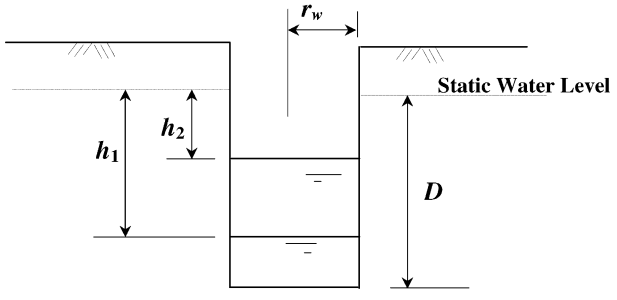

Fig. 12 Schematic diagram for a single auger hole test

The above relationship is known as the Hooghoudt equation, where Δt is the time required to raise the water level from h_1 to h_2. The other notations are showed in Fig. 12.

The second equation was the one revised by Ernst to include the bottom effect:

$$k = \frac{40}{\left(20 + \frac{D}{r_w}\right)\left(2 - \frac{0.5(h_1+h_2)}{D}\right)} \cdot \frac{r_w}{0.5\,(h_1 + h_2)} \cdot \frac{(h_1 - h_2)}{\Delta t} \qquad (3)$$

Table 8 Ineson comparison of yield of boreholes in fissured and porous aquifers

Borehole diameter (m)	0.1	0.2	0.3	0.41	0.46	0.61	0.81	1.01
Fissured non-porous aquifer	0.3	0.62	0.8	0.94	1	1.14	1.28	1.33
Homogeneous porous aquifer	0.56	0.81	0.9	0.98	1	1.04	1.13	1.15

 DOI 10.1007/s10040-002-0205-9

The third equation is the one proposed by the US Department of the Navy:

$$k = \frac{r_w}{16DS} \cdot \frac{(h_2 - h_1)}{\Delta t} \quad \text{for} \quad D/r_w < 50 \tag{4}$$

where, S is the shape factor, which can be estimated from Fig. 13.

Figure 13 is limited to a maximum r_w/D of 0.3; the authors extended the figure through the following correlation:

$$S = A_1 \left(\frac{r_w}{D}\right)^{P_1} \left(A_2 \left(1 - \frac{(h_1 + h_2)}{D}\right)^{P_2} + A_3\right) \tag{5}$$

where A_1=0.135, P_1=–0.628, A_2=–5.137, P_2=2.261 and A_3=5.161, with high coefficient of determination R^2= 0.9976. The calculated coefficients of permeability are presented in Table 9. The Hooghoudt Equation gave different permeability coefficients with the change of water level in the trial pit. This variation is because of the

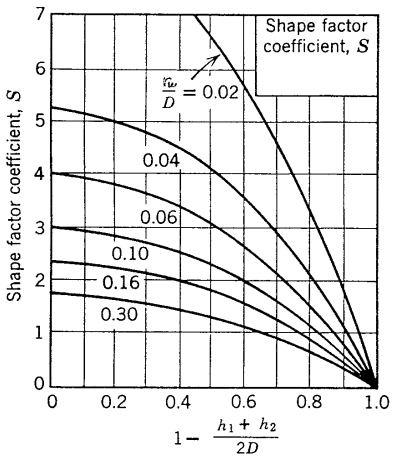

Fig. 13 Shape factor coefficient

Table 9 The calculated coefficient of permeability in the nonsteady-state condition

Water level in pit (m QND)		Delta (t) (min)	h_1 (m)	h_2 (m)	k (m/s)				US Department of the Navy			
					Hooghoudt		Ernst		r_w (same area)		r_w (same perimeter)	
From	To				r_w (same area)	r_w (same perimeter)	r_w (same area)	r_w (same perimeter)	Shape factor	k (m/s)	Shape factor	k (m/s)
–2.820	–2.720	1.50	3.350	3.250	5.81E-03	8.12E-03	1.95E-03	2.41E-03	–	–	–	–
–2.720	–2.620	1.50	3.250	3.150	5.99E-03	8.38E-03	1.95E-03	2.41E-03	–	–	–	–
–2.620	–2.520	1.50	3.150	3.050	6.19E-03	8.65E-03	1.96E-03	2.42E-03	–	–	–	–
–2.520	–2.420	2.00	3.050	2.950	4.80E-03	6.70E-03	1.48E-03	1.82E-03	–	–	–	–
–2.420	–2.220	3.50	2.950	2.750	5.77E-03	8.06E-03	1.71E-03	2.11E-03	–	–	–	–
–2.220	–2.120	2.33	2.750	2.650	4.57E-03	6.39E-03	1.30E-03	1.61E-03	–	–	–	–
–2.120	–2.020	1.92	2.650	2.550	5.76E-03	8.05E-03	1.60E-03	1.98E-03	–	–	–	–
–2.020	–1.920	1.83	2.550	2.450	6.29E-03	8.79E-03	1.71E-03	2.11E-03	–	–	–	–
–1.920	–1.820	1.67	2.450	2.350	7.18E-03	1.00E-02	1.90E-03	2.35E-03	–	–	–	–
–1.820	–1.720	1.50	2.350	2.250	8.34E-03	1.17E-02	2.16E-03	2.67E-03	–	–	–	–
–1.720	–1.620	2.50	2.250	2.150	5.23E-03	7.31E-03	1.33E-03	1.64E-03	–	–	–	–
–1.620	–1.520	2.50	2.150	2.050	5.48E-03	7.66E-03	1.36E-03	1.68E-03	–	–	–	–
–1.520	–1.420	2.00	2.050	1.950	7.19E-03	1.01E-02	1.75E-03	2.15E-03	–	–	–	–
–1.420	–1.320	2.00	1.950	1.850	7.57E-03	1.06E-02	1.80E-03	2.22E-03	–	–	–	–
–1.320	–1.220	1.92	1.850	1.750	8.33E-03	1.16E-02	1.94E-03	2.39E-03	–	–	–	–
–1.220	–1.120	2.00	1.750	1.650	8.46E-03	1.18E-02	1.93E–03	2.38E-03	–	–	–	–
–1.120	–1.020	2.02	1.650	1.550	8.90E-03	1.24E-02	1.99E-03	2.46E-03	0.731	6.52E-05	0.644	9.05E-05
–1.020	–0.920	2.05	1.550	1.450	9.36E-03	1.31E-02	2.05E-03	2.53E-03	0.727	6.46E-05	0.641	8.97E-05
–0.920	–0.820	1.98	1.450	1.350	1.04E-02	1.45E-02	2.23E-03	2.76E-03	0.719	6.76E-05	0.634	9.38E-05
–0.820	–0.720	2.20	1.350	1.250	1.01E-02	1.41E-02	2.12E-03	2.62E-03	0.707	6.19E-05	0.623	8.59E-05
–0.720	–0.620	2.23	1.250	1.150	1.08E-02	1.50E-02	2.23E-03	2.75E-03	0.689	1.25E-04	0.608	1.74E-04
–0.620	–0.520	2.27	1.150	1.050	1.15E-02	1.61E-02	2.35E-03	2.90E-03	0.667	6.36E-05	0.588	8.83E-05
–0.520	–0.420	2.37	1.050	0.950	1.21E-02	1.70E-02	2.43E-03	3.00E-03	0.638	6.37E-05	0.563	8.83E-05
–0.420	–0.320	2.52	0.950	0.850	1.27E-02	1.77E-02	2.49E-03	3.08E-03	0.604	6.33E-05	0.532	8.78E-05
–0.320	–0.220	2.57	0.850	0.750	1.40E-02	1.96E-02	2.70E-03	3.34E-03	0.564	6.65E-05	0.497	9.22E-05
–0.220	–0.120	2.80	0.750	0.650	1.47E-02	2.05E-02	2.79E-03	3.44E-03	0.517	6.65E-05	0.456	9.23E-05
–0.120	–0.020	3.08	0.650	0.550	1.56E-02	2.18E-02	2.91E-03	3.59E-03	0.464	6.73E-05	0.409	9.34E-05
–0.020	0.080	3.33	0.550	0.450	1.73E-02	2.42E-02	3.18E-03	3.92E-03	0.405	7.14E-05	0.357	9.91E-05
0.080	0.180	3.83	0.450	0.350	1.89E-02	2.64E-02	3.40E-03	4.20E-03	0.339	7.42E-05	0.298	1.03E-04
0.180	0.280	4.67	0.350	0.250	2.07E-02	2.90E-02	3.66E-03	4.52E-03	0.266	7.77E-05	0.234	1.08E-04
0.280	0.380	6.17	0.250	0.150	2.38E-02	3.33E-02	4.09E-03	5.05E-03	0.185	8.42E-05	0.163	1.17E-04
0.380	0.480	10.33	0.150	0.050	3.06E-02	4.28E-02	4.81E-03	5.94E-03	0.098	9.51E-05	0.086	1.32E-04
0.480	0.530	14.67	0.050	0.000	6.48E-01	9.06E-01	6.70E-03	8.27E-03	0.028	2.36E-04	0.024	3.28E-04
			Average		3.01E-02	4.20E-02	2.42E-03	2.99E-03		8.32E-05		1.15E-04

 DOI 10.1007/s10040-002-0205-9

oversimplified assumptions made by Hooghoudt, which contradicts the complexity of the investigated strata. Ernst and the US Department of the Navy equations gave almost a constant coefficient of permeability, which can be attributed to the close conformity between their assumptions and the existing natural flow conditions. The average permeability of the last two relations was 2.7×10^{-3} and 1.0×10^{-4} m/s, respectively.

The US Department of the Navy developed the following equation to calculate the coefficient of permeability for cased holes (Das 1987):

$$k = \frac{2\pi r_w + 11L}{11\Delta t} \ln \frac{h_1}{h_2} \quad (6)$$

where the notations are shown in Fig. 14. The estimated permeability coefficients are presented in Table 10. Average vertical permeability is 3.5×10^{-5} m/s.

A comparison between the predictions of Eqs. (2), (3) and (4) is shown in Fig. 15. The predictions of the Hooghoudt equation differed to the measurements by about 100-fold, whereas the Ernest and US Navy equations differed two- to fourfold to the measurements.

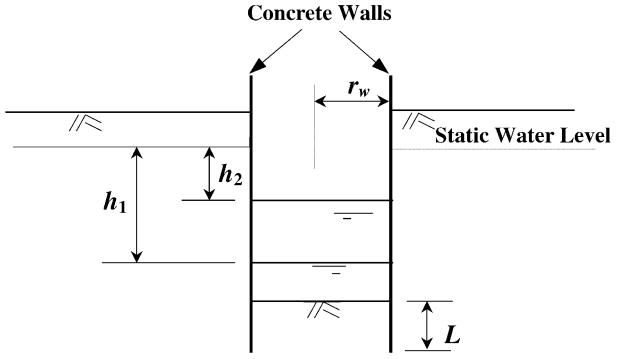

Fig. 14 Schematic diagram for a cased hole

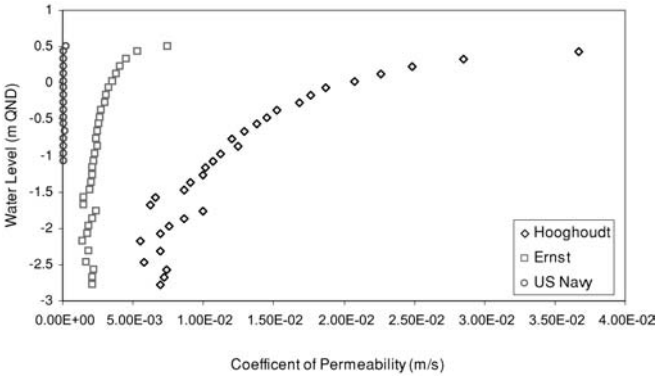

Fig. 15 Coefficient of permeability versus water-table level

Table 10 The calculated vertical coefficient of permeability in the nonsteady-state condition (cased hole)

Water level at trial pit (m QND)		h_1 (m)	h_2 (m)	k (m/s)	
From	To			r_w (same area)	r_w (same perimeter)
–2.820	–2.470	3.350	3.000	4.17E-05	4.60E-05
–2.470	–2.150	3.000	2.680	4.26E-05	4.70E-05
–2.150	–1.890	2.680	2.420	3.85E-05	4.25E-05
–1.890	–1.710	2.420	2.240	2.92E-05	3.22E-05
–1.710	–1.500	2.240	2.030	3.72E-05	4.10E-05
–1.500	–1.370	2.030	1.900	2.50E-05	2.76E-05
–1.370	–1.220	1.900	1.750	3.10E-05	3.43E-05
–1.220	–1.080	1.750	1.610	3.15E-05	3.48E-05
–1.080	–0.930	1.610	1.460	3.69E-05	4.08E-05
			Average	3.48E-05	3.85E-05

Area=15.92 m^2; perimeter=15.96 m; r_w=2.251 m (same area), 2.540 m (same perimeter); L=0.300 (m); Δt=70 min

Conclusions and Recommendations

1. The coefficient of permeability, calculated according to Mansur and Kaufman, Ernst and the US Navy, was affected by the water table level in both steady- and nonsteady-state conditions. This can be explained by the nature of the fissured aquifer and the non-uniform distribution of the flow area.
2. The Hooghoudt equation was used for comparison purposes only and was excluded in the previous analysis due to the high variation (around 100 times) of the value of the coefficient of permeability with the change in water table level. The variation in the case of Ernst and US Navy relations was two- to fourfold only. The incorporation of the shape factor by US Navy has made the use of the equation more applicable for wide field variable conditions. The site conditions in the Doha formation was complicated because of the proximately of the sea level, dictating the variable head. The geology of the area added to the complexity of the hydraulic behaviour of the strata. The presence of many caverns observed in the excavation led to two different types of flow at the same time. A mixed confined and a water table flow condition prevailed because of the presence of pressurised flow through the lower caverns, whereas water table flow existed at the high levels.
3. The obtained value for the vertical coefficient of permeability according to the US Navy (cased hole) was between 4.4×10^{-5} and 3.9×10^{-5} m/s. The variation is minimal and could be explained with reference to the limited interference between the horizontal and vertical flow.
4. The recommended value for the coefficient of permeability depended upon the water table level, which was affected by the tidal condition. Accordingly, the pumping rate should be adjusted during the groundwater modelling for the prediction of the required site dewatering.
5. The computed values of permeability can be compared for various drawdown levels, as shown in Table 11. It is apparent that the method of calculation greatly affects the computed answer. Neither Hooghoudt nor the US Navy formulae give believable

 DOI 10.1007/s10040-002-0205-9

Table 11 Computed values of permeability compared for various drawdown levels

Water level in pit (m QND)	*k* (m/s)		
	M & K (const. head)	Ernst (rising head)	US Navy (rising head)
+0.535	2.18×10^{-4}	8.27×10^{-3}	3.28×10^{-4}
+0.445	5.08×10^{-4}	5.94×10^{-3}	1.32×10^{-4}
–1.320	1.16×10^{-3}	2.22×10^{-3}	–
–1.670	1.62×10^{-3}	1.64×10^{-3}	$\cong5\times10^{-5}$

results. The Mansur and Kaufman equation for steady-state flow and the Ernst equation for nonsteady-state flow agree closely at large values of drawdown.

6. The interaction between fissure flow and rock material flow is complex. The drawdown in the observation well does not respond to the pumping rate (refer to Tables 2 and 3). One presumes the well is not directly connected to the fissure system because there are few in the area. The fissure flow may well respond rapidly to the tidal fluctuations.

References

Akili W, Jackson RM (1998) Shallow foundations on a diagenetic limestone formation in Qatar. International Geotechnical Conference Proceedings, St Louis, paper no 1.41

Arab Center for Engineering Studies (1998) Permeability test report. December, Qatar

BS 8004 (1986) Section six. Geotechnical processes: groundwater lowering, grouting and other methods of changing the groundwater characteristics in situ

Cedergren HR (1989) Seepage, drainage, and flow nets, 3rd edn. Wiley, New York

Das BM (1987) Advanced soil mechanics. McGraw Hill, New York

Department of Civil Aviation and Meteorology (1998) The Doha calendar. Ministry of Communications and Transport, Qatar

Department of the Army, the Navy, and the Air Force (1983) Dewatering and groundwater control. Army TM 5-818-5, Navy NAVFAC p-418, Air Force AFM 88-5, ch 6, Washington

Domenico PA, Schwartz FW (1998) Physical and chemical hydrogeology. Wiley, New York

Driscoll FG (1989) Groundwater and wells, 2nd edn. Johnson Filtration Systems, Minnesota

Fetter CW (1988) Applied hydrogeology, 2nd edn. Merrill, Columbus, OH

Gulf Labs (1998) Report on geotechnical site investigation. May, Qatar

Henry FDC (1986) Deformation and groundwater problems in foundation engineering. In: Henry FDC (ed) The design and construction of engineering foundations, 2nd edn. Chapman and Hall, New York, pp 141–245

Mansur CI, Kaufman RI (1962) Dewatering. In: Foundation engineering. McGraw Hill, New York

Powers JP (1992) Construction dewatering, 2nd edn. Wiley, New York

Powrie W, Preene M (1992) Equivalent well analysis of construction dewatering systems. Géotechnique 42(4):635–639

Preene M, Powrie W (1993) Steady-state performance of construction dewatering systems in fine soils. Géotechnique 43(2):191–205

Qatar Industrial Labs (1998) Geotechnical site investigation report. March, Qatar

Vuković M, Soro A (1992) Hydraulics of water wells – theory and application. Water Resources Publications, Michigan

 DOI 10.1007/s10040-002-0205-9